AMERICAN SOCIETY FOR MICROBIOLOGY | Antimicrobial Agents and Chemotherapy®

ANTIVIRAL AGENTS

Chemically Modified Human Serum Albumin Potently Blocks Entry of Ebola Pseudoviruses and Viruslike Particles

Haoyang Li,[a] Fei Yu,[a] Shuai Xia,[a] Yufeng Yu,[a] Qian Wang,[a] Ming Lv,[c] Yan Wang,[d] Shibo Jiang,[a,b] Lu Lu[a]

Key Lab of Medical Molecular Virology of Ministries of Education and Health, School of Basic Medical Sciences, and Shanghai Public Health Clinical Center, Fudan University, Shanghai, China[a]; Lindsley F. Kimball Research Institute, New York Blood Center, New York, New York, USA[b]; Institute of Basic Medical Sciences, Beijing, China[c]; Shanghai Information Center for Life Sciences, Shanghai Institutes for Biological Sciences, Chinese Academy of Sciences, Shanghai, China[d]

ABSTRACT Ebola virus (EBOV), the causative pathogen of the deadly Ebola virus disease (EVD), can be transmitted via contact with EVD patients, including sexual contact with EVD survivors. At present, no licensed vaccine or therapeutic is available. In this study, we compared eight anhydride-modified proteins for their entry-inhibitory activity against the pseudovirus (PsV) carrying the envelope glycoprotein (GP) of the EBOV Zaire or Sudan species (Zaire PsV and Sudan PsV, respectively). We found that 3-hydroxyphthalic anhydride-modified human serum albumin (HP-HSA) was the most effective in inhibiting the entry of both Zaire PsV and Sudan PsV, with the 50% effective concentration being at the nanomolar level and with HP-HSA being more potent than EBOV-neutralizing antibody MIL77-2 (4G7, a component antibody of the ZMapp drug cocktail). The combination of HP-HSA and MIL77-2 exhibited a synergistic effect. HP-HSA had no obvious *in vitro* or *in vivo* toxicity. The EBOV PsV entry-inhibitory activity of HP-HSA remained intact after storage at 45°C for 8 weeks, suggesting that HP-HSA has the potential for worldwide use, including tropical regions in African countries, as either a therapeutic to treat EBOV infection or a prophylactic microbicide to prevent the sexual transmission of EBOV.

KEYWORDS anhydride-modified protein, Ebola virus, viral entry, therapeutic drug, sexual transmission, microbicide

Received 9 October 2016 **Returned for modification** 9 November 2016 **Accepted** 6 January 2017

Accepted manuscript posted online 6 February 2017

Citation Li H, Yu F, Xia S, Yu Y, Wang Q, Lv M, Wang Y, Jiang S, Lu L. 2017. Chemically modified human serum albumin potently blocks entry of Ebola pseudoviruses and viruslike particles. Antimicrob Agents Chemother 61:e02168-16. https://doi.org/10.1128/AAC.02168-16.

Address correspondence to Shibo Jiang, shibojiang@fudan.edu.cn, or Lu Lu, lul@fudan.edu.cn.

Ebola viruses (EBOVs), which belong to the genus *Ebolavirus*, family *Filoviridae*, can be classified into five distinct species, *Zaire ebolavirus* (ZEBOV), *Sudan ebolavirus* (SUDV), *Bundibugyo ebolavirus* (BDBV), *Tai Forest ebolavirus* (TAFV), and *Reston ebolavirus* (RESTV), which are the causative pathogens of Ebola virus disease (EVD) in humans and nonhuman primates (NHPs) (1). EVD patients usually die from multiorgan failure (hepatic and renal failure) or shock caused by systemic infection (2). Historically, ZEBOV and SUDV have been associated with most EVD outbreaks and cause higher rates of mortality (40 to 90%) than the other Ebola viruses (0 to 25%) (1, 3). During the 2013 to 2016 outbreak caused by the ZEBOV species, 28,616 people were infected, and the death toll reached 11,310, according to the *Ebola Situation Report* (2 June 2016) published by the World Health Organization (WHO) (4). This EVD outbreak has almost been eradicated, but because of reemerging viruses carried by their wild reservoirs in Africa, EBOVs may transmit to humans and spread inadvertently (1, 5). EBOVs are usually transmitted through direct contact with EVD patients, whose body fluids contain high titers of viruses (6, 7). The persistence of EBOV in seminal fluid (SF) of EVD survivors for months (8, 9) and the possibility of sexual transmission (10) have recently been confirmed, indicating that new EVD outbreaks might be ignited by EVD survivors

who have already recovered without any EVD symptoms. In order to save the lives of EVD patients and limit the epidemic scale of EVD outbreaks in the future, specific emergency therapeutic drugs with activity against EBOVs, as well as prophylactic microbicides to prevent sexual transmission, are urgently needed. However, no licensed effective antiviral is currently available (11).

Viral entry and genome replication are two main anti-EBOV targets, and several related antivirals are under investigation in clinical trials. Since the fatality rate is positively correlated with the level of viremia during the disease course (7), neutralizing antibody-based treatment, which targets the viral glycoprotein (GP) and blocks viral replication at the entry step, is considered the most efficient and promising therapy. ZMapp, a drug cocktail composed of neutralizing antibodies, was used as a compassionate therapy during the latest outbreak (12), and it is now undergoing an adaptive randomized clinical trial. It is worth noting that the three antibodies in ZMapp specifically target the GP of ZEBOV (Zaire GP), but they barely provide cross-protection against the GPs of other EBOV species. Although pan-EBOV-neutralizing antibodies have recently been found (13), their application is hindered by the high manufacturing cost and the need for cold-chain storage conditions, which African countries are unable to afford for mass clinical use (14, 15). In addition, several studies have demonstrated that viruses could still be detected in the testes of male survivors for months after hospital discharge, even though their immune systems were able to produce neutralizing antibodies (8, 9, 16, 17). This indicates that the antibody-based therapy cannot eliminate the EBOVs hidden in immune-privileged sites. Two small-molecule-compound drugs approved for use for the treatment of other diseases, bepridil and sertraline, were demonstrated to be EBOV entry inhibitors by targeting host proteins in the endosome (18). Nevertheless, at the dose efficient for anti-EBOV treatment *in vitro*, they still induce cytotoxicity, implying the possibility of side effects *in vivo*. With high expectation, favipiravir and TKM-Ebola, whose mechanisms of action involve interference with the replication and transcription steps in the viral cycle, showed no significant efficacy during clinical use (11, 19, 20). Other immunomodulation or coagulation-regulated drugs, such as type I interferon or recombinant nematode anticoagulant protein c2 (rNAPc2), gave only partial protection to animals in lethal challenge experiments and might disturb the host immune system and metabolism (21, 22).

In our previous studies, we have demonstrated that several kinds of viruses, including human immunodeficiency virus (HIV), human papillomavirus (HPV), and respiratory syncytial virus (RSV), can be inhibited at the viral entry step by anhydride-modified proteins (23–25). Furthermore, one kind of anhydride-modified bovine protein, β-lactoglobulin (β-LG), was clinically applied to treat HPV infection (26). Therefore, we decided to investigate whether anhydride-modified proteins could be utilized as anti-EBOV antivirals. In the present study, we designed and produced a series of anhydride-modified proteins which exhibited remarkable entry-inhibitory activity against pseudotyped EBOVs *in vitro*. Among them, 3-hydroxyphthalic anhydride (HP)-modified human serum albumin (HSA) (HP-HSA) was selected for further research.

RESULTS

HP-HSA was the most potent inhibitor of the entry of both Zaire PsV and Sudan PsV. Anhydride-modified proteins have been identified to be inhibitors of the entry of many enveloped or nonenveloped viruses (23–25, 27). To investigate the inhibitory effects of anhydride-modified proteins on the entry of EBOV pseudovirus (PsV), we constructed a small library of anhydride-modified proteins, including 3-hydroxyphthalic anhydride (HP)-modified human serum albumin (HSA) (HP-HSA), HP-modified β-lactoglobulin (β-LG) (HP-β-LG), HP-modified chicken ovalbumin (OVA) (HP-OVA), HP-modified bovine serum albumin (BSA) (HP-BSA), maleic anhydride (ML)-modified HSA (ML-HSA), ML-modified β-LG (ML-β-LG), succinic anhydride (SU)-modified HSA (SU-HSA), and SU-modified β-LG (SU-β-LG). In alkaline buffer, the anhydrides participated in nucleophilic substitution chemical reactions and formed covalent bonds

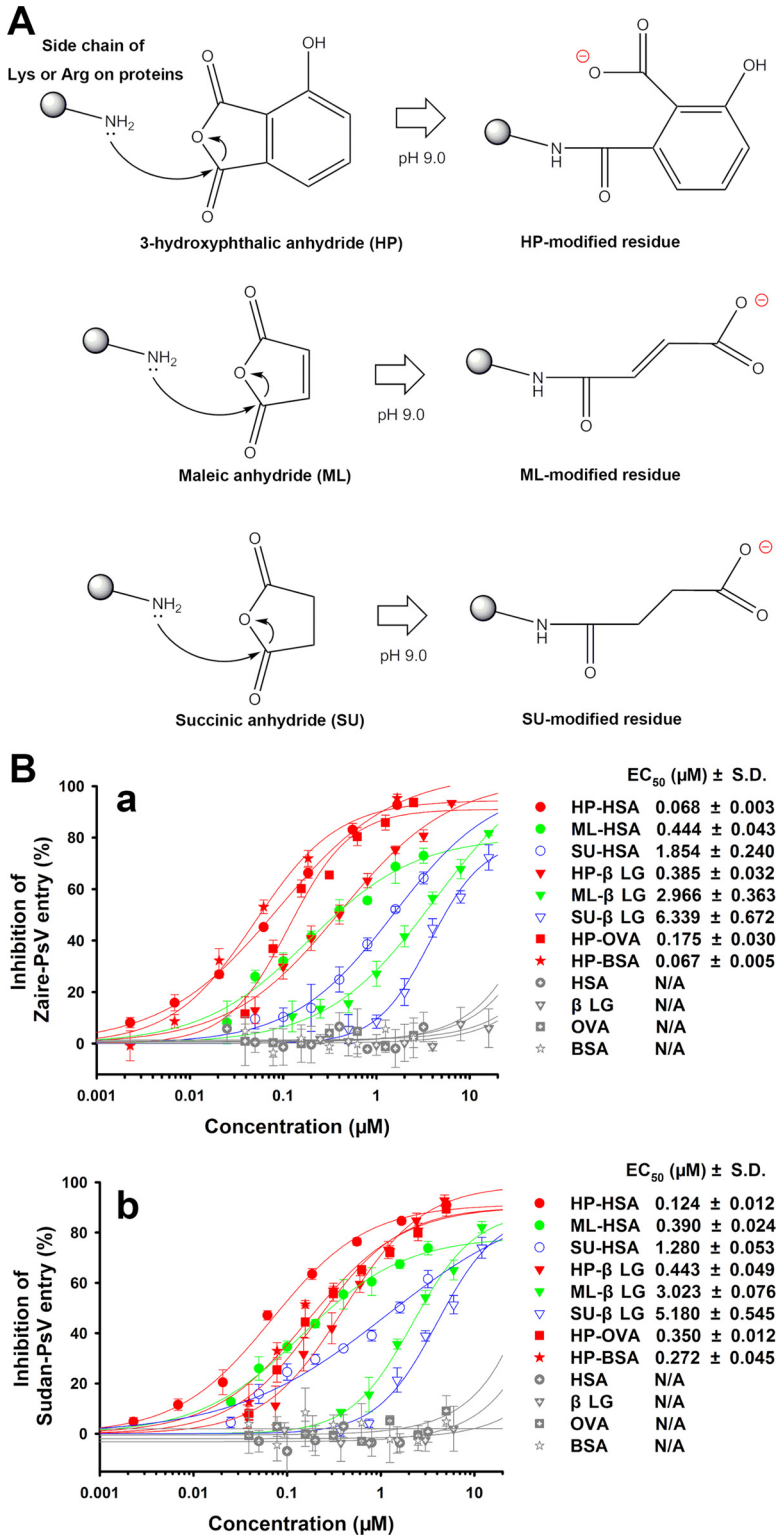

FIG 1 Chemical modification of human and animal proteins and the inhibitory activity of anhydride-modified proteins on EBOV PsV entry. (A) Chemical formulas that represent the nucleophilic substitution chemical reactions on the lysine or arginine residues of proteins. (B) The viral entry-inhibitory activities of anhydride-modified proteins were tested on HuH-7 cells cultured with Zaire PsV (a) or Sudan PsV (b). The results for unmodified proteins, used as negative controls, are also shown. All experiments were performed in triplicate, and the error bars indicate standard deviations.

with the lysine or arginine residues of these original proteins, resulting in reversion of the electrical charges on the residues (Fig. 1A). All anhydride-modified proteins showed activities inhibiting the entry of PsV of EBOV Zaire (Zaire PsV) and EBOV Sudan (Sudan PsV) (Fig. 1B). In particular, the HP-modified proteins exhibited more potent activity than either the ML- or SU-modified proteins, as indicated by the concentrations required for 50% of the maximum effect (EC_{50}s) in Fig. 1B. Among the eight anhydride-modified proteins, HP-HSA was the most potent inhibitor of Zaire PsV and Sudan PsV with EC_{50}s of 0.068 and 0.124 μM, respectively. In contrast, HP-HSA had no effect on the entry of vesicular stomatitis virus (VSV) PsV (see Fig. S1 in the supplemental material). None of the four unmodified proteins inhibited EBOV PsV entry (Fig. 1B), and HSA served as a negative control in subsequent studies. Since EBOVs are blood-borne transmission viruses and severe EVD cases are usually accompanied by heavy viremia (6, 7), the safety of a practical protein-based antiviral when it is infused into blood must be ensured. Therefore, we selected HP-HSA, which was derived from HSA, the most abundant protein in blood, for further study.

The anhydride modification ratio of HSA is critical for HP-HSA's entry-inhibitory activity against EBOV PsV. In previous studies, we demonstrated that the percentage of anhydride-modified residues was proportional to the entry-inhibitory activity of anhydride-modified proteins (23, 25). As shown in Fig. 2A, the modification ratio of alkaline amino acid residues depended on the final concentration of HP in the anhydride reaction system, and the molecular masses of these graded-modified HSAs were also characterized by sodium dodecyl sulfate-polyacrylamide gel electrophoresis (SDS-PAGE) (Fig. 2B). At the final HP concentration of 60 mM, which is also the condition for the generation of HP-HSA, the residues of lysine and arginine on HSA were fully occupied by HP, and its molecular mass reached ~79.9 kDa, identical to that of HP-HSA. We also found that HP-HSA's entry-inhibitory activity against EBOV PsV was positively correlated with the residue modification ratio of HSA (Table 1). When the modification ratios of the residues were below 50%, the EC_{50}s against Zaire PsV or Sudan PsV entry were about or more than 10 μM. In contrast, the EC_{50}s against Zaire PsV entry decreased to 0.087 $\pm$ 0.030 when the modification ratios of lysine and arginine reached 88.3% and 78.1%, respectively. HP-HSA (fully modified HSA; the model as shown in Fig. 2C) displayed the minimum EC_{50} and EC_{90} values. These results verified that the HP modification, together with the modification ratio, was essential for HP-HSA's entry-inhibitory activity against EBOV PsV.

HP-HSA maintained its *in vitro* entry-inhibitory activity against EBOV PsV in human and animal sera as well as in human SF and VFS. Since EBOVs infect tissues and organs via blood circulation, anti-EBOV drug candidates should be delivered into blood and maintain antiviral activity in plasma. Therefore, we tested the Zaire PsV entry-inhibitory activity of HP-HSA in sera from mice, rabbits, monkeys, and humans. As shown in Table 2, the EC_{50} of HP-HSA showed no significant change when it was mixed with serum from different species from that when it was mixed with Dulbecco modified Eagle medium (DMEM), while the EC_{90} values increased slightly, but it still inhibited Zaire PsV entry by 90% at the micromolar scale. Our previous studies demonstrated that anhydride-modified proteins could be utilized as anti-HIV or anti-HPV microbicides (25, 26, 28). In order to determine whether HP-HSA could be developed as an anti-EBOV microbicide against the sexual transmission of EBOV, we tested the antiviral activity of HP-HSA against both Zaire PsV and Sudan PsV entry in human genital fluids, including seminal fluid (SF) and vaginal fluid simulant (VFS). As shown in Fig. S2, HP-HSA showed the same EBOV PsV entry-inhibitory activity after it was premixed with human genital fluids as it did after it was premixed with DMEM as a control. The EC_{50}s of HP-HSA for inhibiting Zaire PsV entry were 0.077 $\pm$ 0.010 μM and 0.101 $\pm$ 0.031 μM in the presence of VFS and human SF, respectively (Table 2). These data demonstrated that HP-HSA could maintain its EBOV PsV entry-inhibitory activity in both serum and genital fluid.

HP-HSA retained its *ex vivo* EBOV PsV entry-inhibitory activity in mouse blood circulation for at least 5 h. To further verify its antiviral activity in blood, we

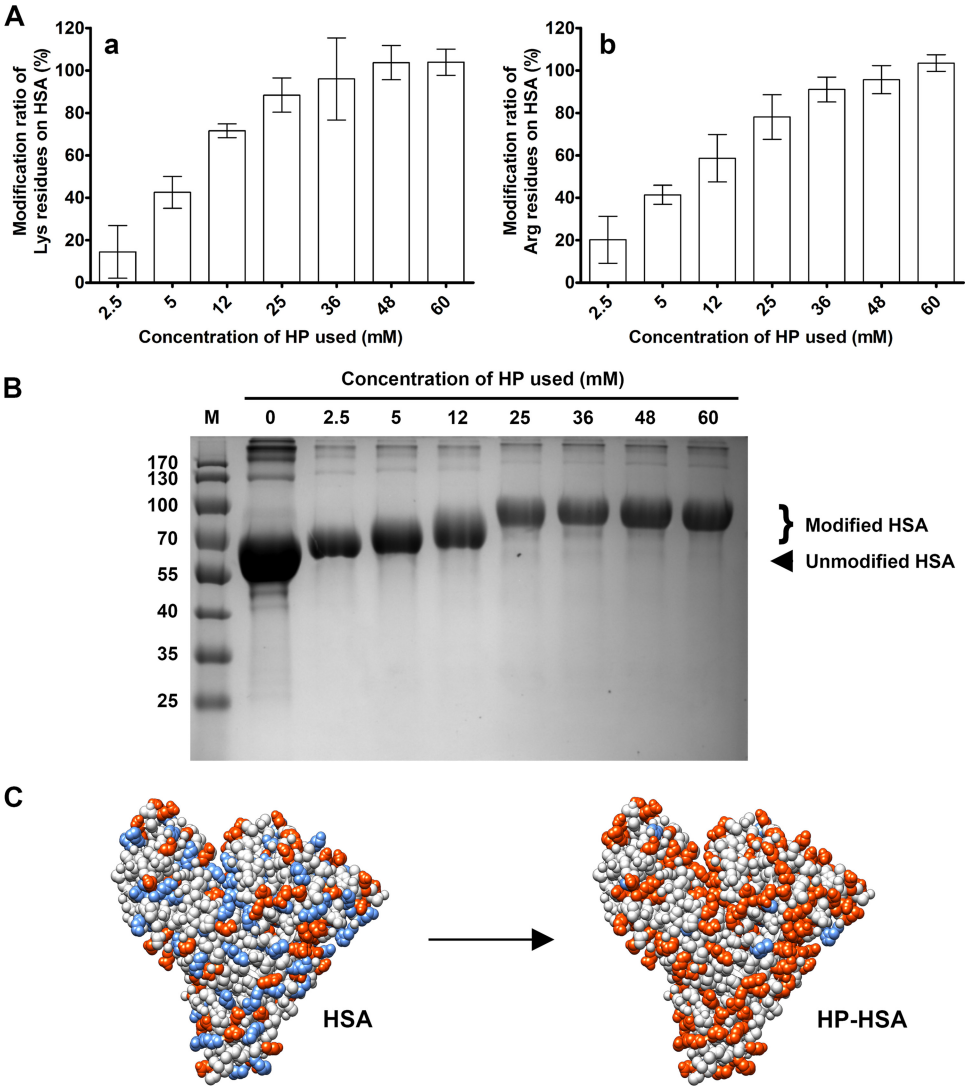

FIG 2 Anhydride modification of HSA and changes to the molecular mass and charge of HP-HSA. (A) The percentage of modified lysine (a) or arginine (b) residues of HSA modified by HP at graded concentrations was quantitated by the TNBS assay or the *ρ*-HPG assay. Experiments were performed in triplicate, and the error bars indicate standard deviations. (B) The molecular masses of HP-modified HSA with different anhydride modification ratios were demonstrated by SDS-PAGE. Lane M, molecular mass markers (the numbers on the left are molecular masses [in kilodaltons]). The molecular mass of unmodified HSA is 66 kDa. (C) The structures (PDB accession number 5ID7) display a change to the charge of HSA before and after HP modification (55). Blue, positively charged residues (lysine, arginine, and histidine); orange, negatively charged residues (aspartic acid, glutamic acid, HP-modified lysine, and arginine).

administered phosphate-buffered saline (PBS), HSA, or HP-HSA to mice by intravenous (i.v.) injection and collected serum at different time points. Serum collected from mice injected with HP-HSA showed more significant Zaire PsV entry-inhibitory activity *in vitro* than serum from the control groups injected with PBS or HSA (Fig. 3). At 1 h postinjection, serum from the low-dose (40 mg/kg of body weight) group still inhibited the entry of Zaire PsV at a dilution of 1:320, while serum from the high-dose (280 mg/kg) group exhibited Zaire PsV entry-inhibitory activity even at a dilution of 1:5,120 (Fig. 3A). At 5 h postinjection, only serum from the high-dose group still showed inhibitory activity (Fig. 3B), which was preserved up to 24 h postadministration (Fig. 3C).

HP-HSA showed no *in vitro* cytotoxicity to HuH-7 cells or *in vivo* acute toxicity to mice. To study the safety of HP-HSA, HuH-7 cells were treated with different concentrations of HP-HSA and assayed for viability. As shown in Fig. 4A, more than 90% of HP-HSA-treated HuH-7 cells remained viable when they were treated with HP-HSA at

TABLE 1 Comparison of EBOV PsV entry-inhibitory activities of HP-HSA modified with different concentrations of HP[a]

HP concn (mM)	Modification rate (%)		Zaire PsV		Sudan PsV	
	Lys	Arg	EC_{50} (μM)	EC_{90} (μM)	EC_{50} (μM)	EC_{90} (μM)
0	0	0	>20	>20	>20	>20
2.5	14.4	20.2	>20	>20	>20	>20
5	42.5	41.4	8.17 ± 1.22	>20	10.63 ± 8.94	>20
12	71.5	58.6	0.643 ± 0.232	>20	2.33 ± 0.54	>20
25	88.3	78.1	0.087 ± 0.030	5.256 ± 0.803	0.172 ± 0.038	6.186 ± 0.424
36	95.9	91.0	0.073 ± 0.019	1.970 ± 0.235	0.105 ± 0.010	4.663 ± 0.068
48	100	95.6	0.096 ± 0.002	1.413 ± 0.086	0.093 ± 0.007	4.433 ± 0.396
60	100	100	0.087 ± 0.011	1.126 ± 0.079	0.088 ± 0.020	2.790 ± 0.539

[a]Each sample was tested in triplicate. Data are presented as the mean ± standard deviation.

a concentration of 100 μM, which is more than 70 times higher than its EC_{90} for inhibiting Zaire PsV entry, and no significant difference in viability from that of HSA-treated HuH-7 cells was noted. To investigate its toxicity *in vivo*, mice were administered PBS, HSA, low-dose HP-HSA (40 mg/kg), and high-dose HP-HSA (280 mg/kg) i.v. as indicated above for the activity study, and their weight changes were recorded for 4 weeks after administration. The mice from both the high-dose and low-dose HP-HSA groups lived normally without any obvious functional disorder, and no difference in weight loss compared with that for mice from the PBS and HSA groups was seen (Fig. 4B). Mice from all four groups were dissected after euthanasia at day 28 postadministration, and neoplasms were not observed either in the functional organs (liver, heart, and kidney) of the circulation system or in the skin and muscle tissues. To verify any cell-level damage in organs after administration, we carried out microimaging of the livers and kidneys of the mice from the four groups after staining with hematoxylin and eosin (H&E). Similar to the results seen for the PBS and HSA groups, the tissue structures of the livers and kidneys from mice in both the low- and high-dose HP-HSA groups were intact. In addition, no obvious inflammatory injury in the kidneys and livers was observed after HP-HSA administration (Fig. 4C). These results suggest no obvious *in vitro* or *in vivo* toxicity of HP-HSA.

HP-HSA exhibited prominent thermostability. Thermostability is a crucial requirement for anti-EBOV drugs, in particular because they will be abundantly used in West and Middle Africa where advanced cold-chain storage, which is especially critical for protein-based drugs, is not readily available (14). Therefore, the thermostability of HP-HSA must be guaranteed. With this aim in mind, HP-HSA stocks diluted in PBS were stored at 4, 25, 37, or 45°C for 8 weeks, and the antiviral activity of HP-HSA at a final concentration of 2.5 μM was tested at different time points. Similar to the findings of our previous studies (23), HP-HSA maintained its EBOV PsV entry-inhibitory activity at temperatures of 4, 25, and 37°C (Fig. 4D). Surprisingly, HP-HSA also exhibited stable activity after storage at 45°C for 2 months or at 4°C for 1 year. The EC_{50} and EC_{90} values of HP-HSA stored in PBS at 4°C for 12 months were 0.086 ± 0.011 μM and 1.511 ± 0.159

TABLE 2 Inhibitory activity of HP-HSA against Zaire PsV when diluted in different body fluids[a]

Reagent used for HP-HSA dilution	EC_{50} (μM)	EC_{90} (μM)
DMEM	0.074 ± 0.003	1.194 ± 0.146
Human serum	0.103 ± 0.019	2.637 ± 0.349
Monkey serum	0.121 ± 0.007	1.170 ± 0.120
Rabbit serum	0.124 ± 0.021	4.733 ± 0.649
Mouse serum	0.074 ± 0.012	2.953 ± 0.263
Human vaginal fluid simulant	0.077 ± 0.010	1.373 ± 0.742
Human seminal fluid	0.101 ± 0.031	2.465 ± 0.727

[a]Each sample was tested in triplicate, and the experiment was repeated two times. Data are presented as the mean ± standard deviation.

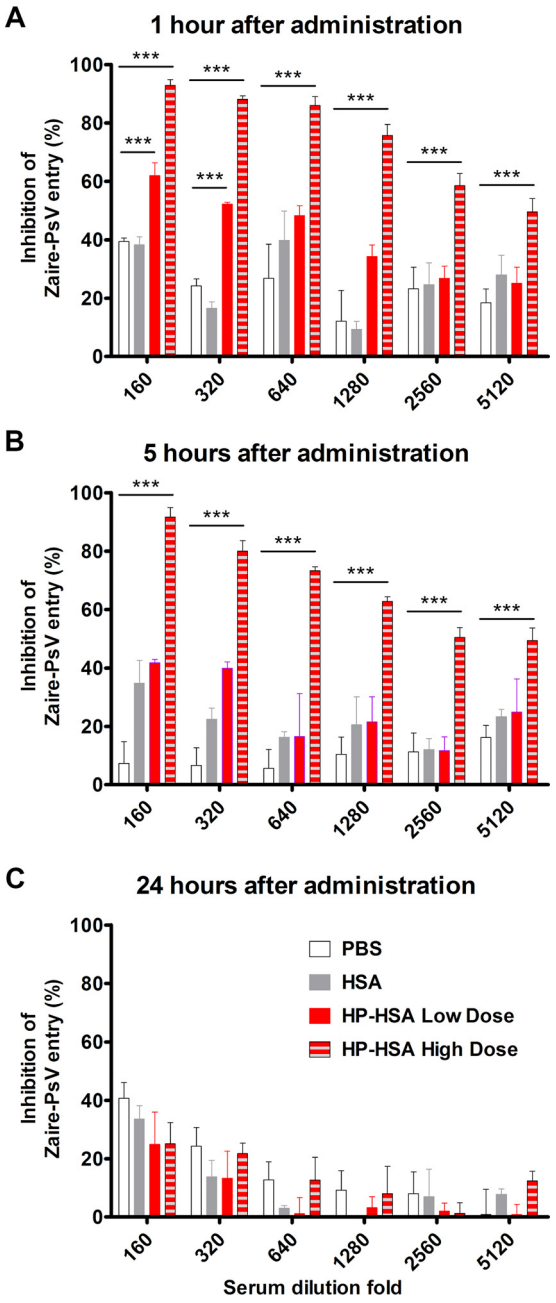

FIG 3 *Ex vivo* Zaire PsV entry-inhibitory activity of HP-HSA in mouse blood circulation. Four groups of female ICR mice were administered PBS (100 μl), HSA in PBS (280 mg/kg), or HP-HSA in PBS (40 mg/kg for the low dose and 280 mg/kg for the high dose) through intravenous injection. Serum was collected at 1 h (A), 5 h (B), and 24 h (C) postadministration, and the entry-inhibitory activity was tested by the Zaire PsV entry assay. All experiments were performed in triplicate, and the error bars indicate standard deviations. The asterisks represent significant differences. ***, $P < 0.001$.

μM, respectively. This prominent thermostability shows that HP-HSA has the potential for application in West and Middle Africa, where extreme weather conditions are commonplace.

HP-HSA inhibited Zaire PsV entry at the early stage and exhibited an affinity for binding to the purified Zaire GP trimer *in vitro*. A time-of-addition assay was performed to explore the potential step of EBOV entry targeted by HP-HSA. As shown in Fig. 5A, when 5 μM HP-HSA was added to HuH-7 cells within 1 h after addition of Zaire PsV, its inhibitory activity was maintained at more than 90%. No significant

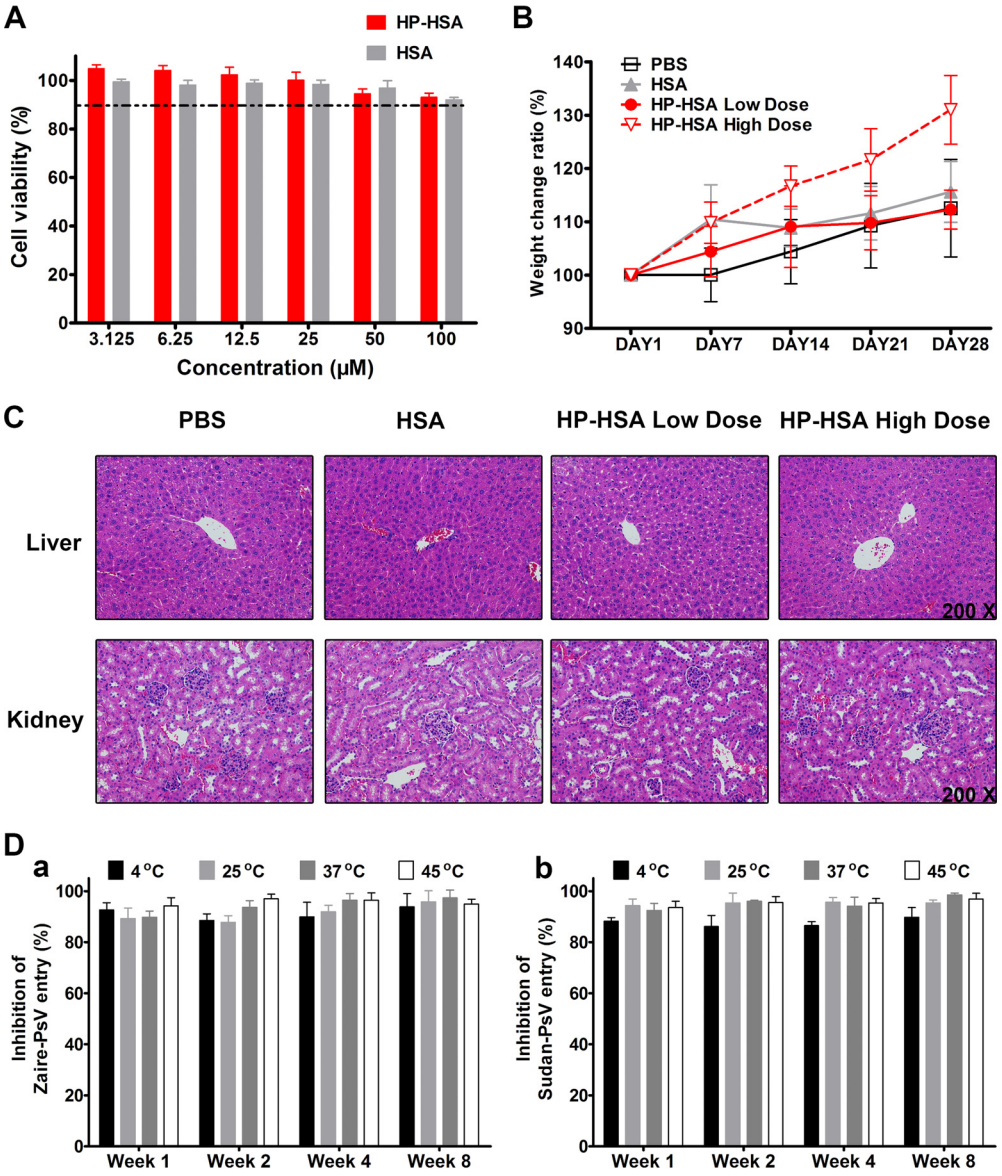

FIG 4 Cytotoxicity *in vitro* and acute toxicity *in vivo* of HP-HSA and its thermostability. (A) The cytotoxicity of HP-HSA or unmodified HSA to HuH-7 cells was determined by a cytotoxicity assay. (B) The weight change ratios for mice treated as described in the legend to Fig. 3 were recorded up to day 28 postinjection. The error bars indicate standard deviations. (C) The structures of H&E-stained sections of livers and kidneys were determined at day 28 postinjection. (D) HP-HSA-treated samples were stored in PBS at different temperatures (4, 25, 37, or 45°C) for 1 to 8 weeks before their inhibition of Zaire PsV (a) or Sudan PsV (b) entry into HuH-7 cells was evaluated. Especially, 45°C was reported to be the highest temperature recorded in all cities in Africa in 2014 (as reported by the Weather China website [http://www.weather.com.cn/]). All experiments were performed in triplicate, and the error bars indicate standard deviations.

difference from the premixed condition (at −0.5 h, when HP-HSA was mixed with Zaire PsV for 0.5 h before addition to HuH-7 cells) was observed. With the delay of the time of addition, the entry-inhibitory activity of HP-HSA gradually decreased and dropped to 40% when HP-HSA was added 8 h later. This result indicates that HP-HSA inhibits Zaire PsV entry at the early stage.

Next, we performed two kinds of binding assays directed toward host factors and viral proteins, respectively. In the time-of-removal assay, HuH-7 cells were incubated with HP-HSA or HSA at 37°C for 1 h and washed with DMEM before Zaire PsV was added. As shown in Fig. 5B, HP-HSA could fully inhibit Zaire PsV entry when the cells were not washed (column 1) but nearly lost its inhibitory ability when it was washed

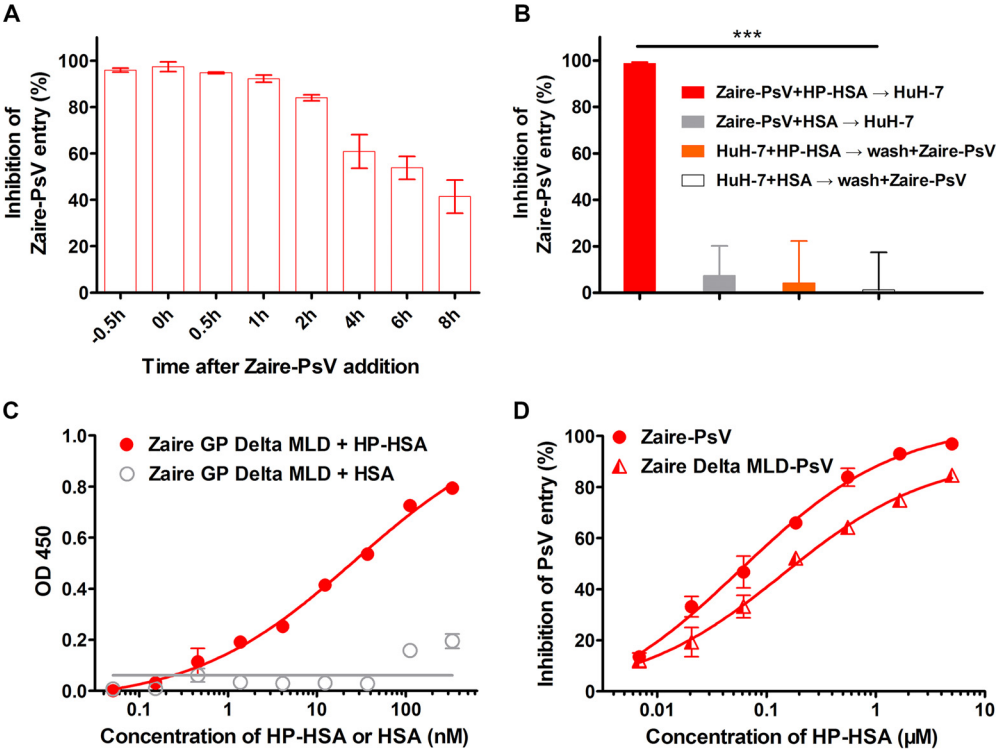

FIG 5 HP-HSA inhibition of Zaire PsV entry at different intervals after addition of PsVs and its affinity of binding to purified Zaire GP trimer *in vitro*. (A) The inhibitory activity of 5 μM HP-HSA at 0, 0.5, 1, 2, 4, 6, and 8 h after Zaire PsV addition was compared with that of HP-HSA premixed with Zaire PsV 0.5 h before PsV addition. (B) HuH-7 cells were incubated with HP-HSA or HSA at 37°C for 1 h and washed with DMEM before Zaire PsV was added. As controls, HP-HSA or HSA was premixed with Zaire PsV before addition into wells plated with HuH-7 cells. (C) The binding affinities of Zaire GP (after the deletion of aa 314 to 462 and aa 637 to 676) and HP-HSA were demonstrated by using a binding ELISA and compared with the binding affinity of unmodified HSA. OD 450, optical density at 450 nm. (D) The entry-inhibitory activity of HP-HSA for Zaire PsV from which the GP MLD was deleted and wild-type Zaire PsV, which was utilized as a control. All experiments were performed in triplicate, and the error bars indicate standard deviations. The asterisks represent significant differences. ***, $P < 0.001$.

away before addition of PsV (column 3). With or without washing, HSA exhibited no inhibitory activity (Fig. 5B, columns 2 and 4). These results indicate that the inhibition of viral entry by HP-HSA is not dependent on a putative interaction with host cell factors. The soluble Zaire GP (without the mucin-like domain [MLD] and the transmembrane [TM] domain) overexpressed on HEK293T cells possesses the native trimer conformation of GP, according to previous observations (29). The conformation was further verified by an enzyme-linked immunosorbent assay (ELISA) for GP binding to MIL77 antibodies, in that two distinct conformational epitopes could be recognized by the MIL77 antibody, MIL77-2 and MIL77-3, respectively (Fig. S3A) (30). The results showed that HP-HSA exhibited a higher affinity of binding to the trimeric GP protein than HSA did (Fig. 5C), suggesting that HP-HSA inhibited the entry of Zaire PsV through a direct interaction with GPs. We then used the Zaire pseudovirus from which the GP MLD was deleted (Zaire delta MLD PsV) to further verify whether the protein interaction was really related to the entry-inhibitory activity. As shown in Fig. 5D, HP-HSA inhibited the entry of Zaire delta MLD PsV. However, a higher concentration of HP-HSA was needed to achieve an inhibitory effect equal to that against Zaire PsV. This result suggests that the interaction between HP-HSA and GP (without MLD) is critical for viral entry inhibition and the existence of MLD may consolidate the binding of the complex.

HP-HSA exhibited more potent Zaire PsV entry-inhibitory activity than other entry inhibitor-based antivirals and exhibited a synergistic effect in combination with neutralizing antibody. Using the Zaire PsV entry inhibition assay, we compared the inhibitory ability of HP-HSA with those of four anti-EBOV drug candidates under development. First, we tested two antibody-based antivirals, MIL77-2 and MIL77-3,

TABLE 3 Comparison of Zaire PsV entry-inhibitory activity of HP-HSA with that of other entry-inhibitory antivirals[a]

Inhibitor	EC_{50} (μM)	EC_{90} (μM)
HP-HSA	0.080 ± 0.015	1.576 ± 0.249
Sertraline	0.477 ± 0.096	2.311 ± 0.146
Bepridil	1.676 ± 0.080	5.046 ± 0.443
MIL77-2 (4G7)	0.258 ± 0.059	8.244 ± 2.373
MIL77-3 (13C6)	>2.5	>10

[a]Each sample was tested in triplicate, and the experiment was repeated three times. Data are presented as the mean ± standard deviation.

which block viral entry by targeting two different sites on the Zaire GP (30, 31). Then, we tested two small-molecule compounds, bepridil and sertraline, which have been considered inhibitors of EBOV function before or at the fusion step (18). As shown in Table 3, HP-HSA exhibited more potent Zaire PsV entry-inhibitory activity (lower EC_{50}s and EC_{90}s) than any of the drug candidates noted above. The EC_{50} and EC_{90} values of HP-HSA were 3- and 8-fold lower than those of MIL77-2, respectively. These results suggest that HP-HSA has the potential to be further developed as a new antiviral for the treatment and prevention of EBOV infection.

To further determine whether HP-HSA could inhibit Zaire PsV entry in synergy with MIL77 antibodies, the inhibitory activities of the inhibitors tested alone or in combination were calculated and compared (Table 4). The combination of HP-HSA with MIL77-2 exhibited potent synergy, with the combination index (CI; representing the level of synergistic effect) being 0.426. The EC_{50} of HP-HSA and MIL77-2 in combination was significantly lower than the EC_{50} of each inhibitor alone, with the dose reductions being 4.72- and 3.11-fold, respectively. Interestingly, the combination of HP-HSA with MIL77-3 showed stronger synergy (CI = 0.223), with the dose reductions being 3.71- and >146-fold, respectively. These results suggest that HP-HSA and MIL77 neutralizing antibodies can be used in combination for the synergistic inhibition of EBOV infection.

HP-HSA inhibited Zaire VLP entry by blocking cell surface attachment. It has been demonstrated that EBOV GP-mediated viral entry consists of at least five steps, including cell surface attachment, endocytosis, cathepsin cleavage of GP, fusion receptor binding, and membrane fusion (32–35). The results of the time-of-addition assay in Fig. 5A indicate that HP-HSA inhibits the entry of Zaire PsV at an early step. To determine which step may be the target for HP-HSA, fluorescent protein-labeled viruslike particles (VLPs) of ZEBOV (Zaire VLPs) were introduced. Recombinant EBOV VLPs, which are morphologically similar to authentic EBOV virions, have been extensively utilized in EBOV research, such as in studies of virion morphology and the viral entry mechanism and in drug development studies, as credible substitutes for infectious EBOVs (32, 36–40).

mCherry-labeled Zaire VLPs were produced as previously described (36–38). An ELISA was performed to confirm the native conformation of the Zaire GPs displayed on the surface of concentrated VLPs (Fig. S3B). After incubation at 37°C with Zaire VLPs, the fluorescent signals from VLPs that entered HuH-7 cells could be detected and digitized by laser scanning confocal microscopy (LSCM) (Fig. S3C). We then collected the emission light signals of mCherry from VLPs incubated in HuH-7 cells treated or not treated with an inhibitor and analyzed three random visual fields for each sample. The

TABLE 4 Inhibitory activity of HP-HSA and MIL77 when used alone or combined against Zaire PsV[a]

	EC_{50} (μM)		Dose reduction		EC_{50} (μM)		Dose reduction	
Inhibitor A	Alone	In combination	(fold)	Inhibitor B	Alone	In combination	(fold)	CI
HP-HSA	0.103 ± 0.023	0.018 ± 0.003	4.72	MIL77-2	0.222 ± 0.010	0.054 ± 0.010	3.11	0.426 ± 0.106
HP-HSA	0.080 ± 0.015	0.017 ± 0.0002	3.71	MIL77-3	>2.5	0.017 ± 0.0002	>146	0.223 ± 0.048

[a]Each sample was tested in triplicate, and the experiment was repeated two times. Data are presented as the mean ± standard deviation.

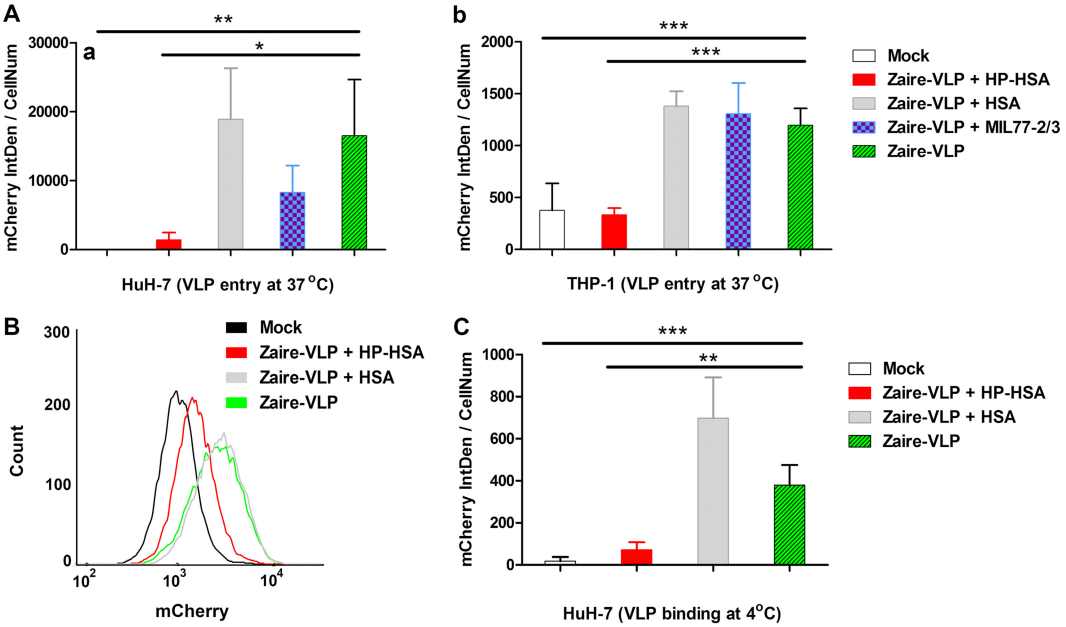

FIG 6 The entry-inhibitory activity of HP-HSA for Zaire VLPs. (A) The fluorescent density (per cell) integrated into HuH-7 cells (a) or differentiated THP-1 cells (b) cultured with mCherry-labeled Zaire VLPs at 37°C for 6 to 8 h (treated with or without an inhibitor) was analyzed and compared. (B) Flow cytometry results for mCherry-labeled Zaire VLPs that entered HuH-7 cells (treated with HP-HSA or HSA). (C) The fluorescent integrated density (per cell) of HP-HSA-treated HuH-7 cells was analyzed to determine VLP entry after a temperature shift assay. The data in each column were calculated from three random visual fields. The error bars indicate standard deviations, and asterisks represent significant differences. *, $P < 0.05$; **, $P < 0.01$; ***, $P < 0.001$. mCherry IntDen, mCherry integrated density; CellNum, cell number.

results showed that the density of fluorescent mCherry integrated into HP-HSA-treated cells was significantly less than that of mCherry integrated into cells treated or not treated with HSA or MIL77 antibodies (Fig. 6Aa).

Human macrophages are the primary target cells during the early course of EVD (3). In agreement with the result derived from HuH-7 cells, HP-HSA also blocked the entry of Zaire VLPs into differentiated THP-1 cells (representing human macrophages) (Fig. 6Ab), and it showed no obvious cytotoxicity to THP-1 cells (Fig. S4). All of the raw images used in the analysis are presented in Fig. S5.

The flow cytometry (FCM) results for HuH-7 cells showed that 23.4% of untreated cells and 26.1% of HSA-treated cells were mCherry positive, while only 2.5% of HP-HSA-treated cells were mCherry positive (Fig. 6B; see also Fig. S6). The signals for the entry of the VLPs into differentiated THP-1 cells were too weak to be measured by FCM (data not shown). These results indicate that HP-HSA inhibits VLP entry before the VLP enters the endosome, and thus, the step of VLP attachment or endocytosis may be the target for HP-HSA.

EBOVs or EBOV VLPs enter the endosome by macropinocytosis (32, 41), and this kind of endocytosis depends on actin polymerization and consumes energy (42). At 4°C, the speed of actin polymerization or depolymerization becomes significantly lower than that at the physiological temperature (43). However, the interaction between virions and host factors on the cell surface is not blocked by a lower temperature. Therefore, we incubated VLPs and HuH-7 cells at 4°C so that VLPs could bind to the cell surface and washed away unbound VLPs before shifting the cells to 37°C for further incubation. The integrated fluorescent density of the cells treated with HP-HSA was significantly lower than that of cells treated or not treated with HSA (Fig. 6C), indicating that HP-HSA blocked Zaire VLP entry at the attachment step of viral entry.

To sum up the mechanism studies based on both EBOV PsV and EBOV VLP entry assays, we conclude that HP-HSA inhibits EBOV GP-mediated viral entry at the cell surface attachment step by directly interacting with EBOV GP.

DISCUSSION

Although they are believed to be the most promising antivirals against EBOVs, neutralization antibody-based drugs may not be widely used in Africa as a result of their high cost and rigorous storage conditions (14, 15). Small-molecule drugs, like bepridil or sertraline, may cause side effects since they show cytotoxicity to cultured cells (18). Furthermore, to date, no drug candidate has been designed to block EBOV sexual transmission, which is a novel EBOV transmission pathway (10). Therefore, therapeutic drugs which can be safely used for EVD patients and prophylactic medicines that prevent sexual transmission should be prepared before the next outbreak.

Combined with our previous research, we designed and compared the EBOV PsV entry-inhibitory activities of eight anhydride-modified proteins in this study, and we focused on HP-modified HSA because it potently inhibited the cell entry of both Zaire PsV and Sudan PsV. As a drug candidate for anti-EBOV therapeutic treatment, HP-HSA should be delivered into blood. Our research demonstrated that HP-HSA maintained its EBOV PsV entry-inhibitory activity in serum *in vitro* and *ex vivo* without any obvious toxicity to cultured cells or treated mice. Besides, HP-HSA inhibited the entry of Zaire VLPs into both HuH-7 cells and differentiated human THP-1 cells, indicating that HP-HSA might prevent EBOV infection of both liver cells and macrophages *in vivo*, cells that are crucial targets during EBOV infection (3).

Highly pure (>99%) recombinant HSA can expediently be obtained from transgenic rice seeds (2.75 g HSA per kg of brown rice) (44), making it possible to produce HP-HSA on a large scale. In contrast, for antibody production in plants, which is the cheapest approach to antibody production, only 500 mg antibody per kg of fresh biomass of *Nicotiana benthamiana* leaves can be prepared (45). HP-HSA also exhibited a synergistic effect with the EBOV-neutralizing antibody. We thus suggest that HP-HSA could be administered alone or along with EBOV-neutralizing antibodies to reduce the dosage of antibodies and minimize the cost, as well as increase the overall genetic barrier of therapy against antibody-resistant EBOV variants. The thermostability of HP-HSA also allows it to be stored over the long term as emergency anti-EBOV stocks in African countries, especially rural areas, which might otherwise lack cold storage conditions.

On the other hand, the persistence and sexual transmission of EBOV have attracted more and more attention (8–10, 16, 17). Male Ebola survivors may not eliminate viruses from their testicles during the first few months after discharge from the hospital, and about 74% of male survivors reported that they did not use condoms during sexual intercourse (16). Therefore, an effective and safe microbicide is urgently needed. We identified that HP-HSA maintained its *in vitro* EBOV PsV entry-inhibitory activity in human SF and VFS. Actually, anhydride-modified proteins, such as anhydride-modified bovine β-lactoglobulin, have been studied and utilized as microbicides against HIV and HPV in clinics for years, and their effectiveness and safety as drugs have been verified (26, 28). Our present study suggests that HP-HSA can also be developed as a prophylactic microbicide for people who have recovered from EBOV infection but can still transmit the virus to their sexual partners.

The GP of EBOV has been considered the only viral factor that mediates viral entry (3, 35). We have demonstrated that HP-HSA can directly bind to GP and block the entry of EBOV PsV into cells. Taking into consideration the points of previous research (23, 25, 27, 46), we speculated that HP-HSA inhibited virus entry by blocking the interaction between EBOV GP and host factors on the cell surface that facilitate viral entry. Accordingly, we used mCherry-labeled EBOV VLPs to further verify that HP-HSA may target the first step (attachment) of viral entry. This target is different from the target of MIL77 antibodies, which exhibited antiviral activity in the endosome before membrane fusion (40), and this result may account for the synergistic effect between HP-HSA and MIL77 antibodies.

The HP modification confers on HP-HSA a negatively charged surface under the physiological pH condition. Thus, this charge effect might account for the antiviral activity of HP-HSA since unmodified HSA did not show either an affinity of binding to

GP or entry-inhibitory activity against EBOV PsVs or EBOV VLPs. A study of the EBOV GP structure has pointed out the presence of more positive charge on the surface of Zaire EBOV GP than on that of Sudan EBOV GP (47), which is consistent with the finding that HP-HSA was more effective against Zaire PsV than Sudan PsV.

In conclusion, we have identified HP-HSA to be a potent and safe inhibitor of the entry of EBOV PsVs and EBOV VLPs by blocking the attachment step. It can be further developed as either a therapeutic medicine for the treatment of EVD patients or a prophylactic microbicide for the prevention of EBOV sexual transmission. Its prominent thermostability endows HP-HSA with the potential for widespread use in African countries and worldwide to save lives during the next EBOV outbreak. Therefore, its further development is warranted.

MATERIALS AND METHODS

Reagents. 3-Hydroxyphthalic anhydride (HP), succinic anhydride (SU), maleic anhydride (ML), 2,4,6-trinitrobenzenesulfonic acid (TNBS), human serum albumin (HSA), β-lactoglobulin (β-LG), chicken ovalbumin (OVA), bovine serum albumin (BSA), bepridil hydrochloride (bepridil), sertraline hydrochloride (sertraline), and dimethyl sulfoxide (DMSO) were purchased from Merck (Germany). ρ-Hydroxyphenylglyoxal (ρ-HPG) was purchased from Thermo Fisher Scientific (USA). Goat anti-human serum albumin antibody and horseradish peroxidase (HRP)-conjugated goat anti-human IgG antibody were purchased from Abcam (UK). HRP-conjugated rabbit anti-goat IgG antibody was purchased from Dako (Denmark). The chimeric antibodies MIL77-2 and MIL77-3, which contain the variable regions of 4G7 and 13C6 (the component antibodies of ZMapp), respectively (31), were produced by the Institute of Basic Medical Sciences, Beijing, People's Republic of China. Human serum was purchased from MRC Biological Technologies (China). Serum was prepared from naive female ICR mice, New Zealand rabbits, and rhesus macaques. These animal serum samples were obtained from the Department of Laboratory Animal Science, Fudan University. Human seminal fluid (SF) was purchased from Lee BioSolutions. Inc. (USA).

Plasmids and cells. HEK293T, THP-1, and HuH-7 cells were obtained from the cell bank of the Chinese Academy of Sciences (www.cellbank.org.cn). Human monocyte-derived THP-1 cells were differentiated into macrophages by using phorbol-12-myristate-13-acetate (PMA; Sigma) before they were used as target cells (48). Plasmid pcDNA3.1(+) was purchased from Thermo Fisher Scientific (USA). Plasmid pNL4-3.Luc.R$^-$E$^-$ was obtained from the National Institutes of Health (NIH) AIDS Research and Reference Reagent Program. The coding sequences of the glycoproteins (GPs) of ZEBOV (GenBank accession number KM034549.1) and SUDV (GenBank accession number KC545389.1) were optimized and synthesized by Genewiz Inc. and then cloned into the pcDNA3.1(+) expression vector. Another pcDNA3.1(+) vector containing the ZEBOV GP sequence without the mucin-like domain (MLD; amino acids [aa] 314 to 462) was also constructed. The signal peptides of the EBOV GPs were replaced by an Ig kappa signal peptide. The pMD2.G plasmid containing the sequence of the vesicular stomatitis virus (VSV) G protein was preserved in our laboratory at Fudan University. The DNA sequence of ZEBOV matrix protein VP40 was also synthesized with or without the mCherry sequence at the N terminus as described previously (36, 37) before it was inserted into pcDNA3.1(+). In a soluble expression version of Zaire GP, the coding sequences of the MLD (aa 314 to 462) and transmembrane (TM) domain (aa 637 to 676) were deleted and replaced by a hemagglutinin (HA) tag or a His tag, respectively. The soluble GP protein was produced from HEK293T cells and purified with Ni-Sepharose.

Chemical modification and characterization of anhydride-modified proteins. Anhydride-modified proteins were produced as previously described (23, 25). Briefly, each kind of protein was dissolved with 0.1 M phosphate buffer (pH 8.5) at a final concentration of 20 mg/ml. Afterwards, protein solutions were mixed with different sorts of anhydrides (HP, ML, or SU at 1 M in DMSO) to a final concentration of 60 mM by the addition of five equal aliquots at 20-min intervals, while the pH was adjusted to 9.0 with 4 M NaOH after each mixing. All mixtures were kept at 25°C for two more hours and then dialyzed against PBS. Especially, to obtain a series of HP-modified HSA mixtures with different anhydride modification ratios, HSA was reacted with 0, 2.5, 5, 12, 25, 36, 48, or 60 mM HP anhydride.

The concentration of proteins was measured with a Pierce bicinchoninic acid assay kit (Thermo Fisher Scientific, USA). To determine the percentage of modified lysine or arginine residues in anhydride-modified proteins, a TNBS assay or ρ-HPG assay was performed as previously described (23, 24). The anhydride modification ratio was also visualized by sodium dodecyl sulfate-polyacrylamide gel electrophoresis (SDS-PAGE).

Production of pseudoviruses and entry inhibition assays. Lentivirus-based pseudotypes of EBOVs, which represent the entry process of authentic EBOVs, have been used in basic or antiviral studies for many years (49, 50). The Zaire pseudovirus (Zaire PsV), Sudan pseudovirus (Sudan PsV), Zaire pseudovirus from which the GP MLD was deleted (Zaire delta MLD PsV), and VSV pseudovirus (VSV PsV) were produced by cotransfecting plasmids carrying surface glycoproteins with pNL4-3.Luc.R$^-$E$^-$ as described previously (50). The pseudoviruses in the supernatant were collected 72 h after transfection. The pseudoviruses were quantitated by determination of the level of the lentivirus p24 antigen by ELISA as described previously (51, 52). Liver cells are severely damaged by EBOV infection, which usually causes organ failure during the late course of EVD (3); therefore, the human hepatocyte-derived HuH-7 cell line was selected as the target cell of pseudoviruses. Eight hours before entry inhibition assays, HuH-7 cells

were plated in each well of 96-well plates at a concentration of 10,000 cells per well. The pseudovirus and serial dilutions of the drug candidates were premixed and incubated for 30 min at room temperature before the mixture was added to the HuH-7 cells. The mixture of an inhibitor and pseudovirus in each well was replaced by fresh medium 16 h after addition of PsV. Transduced HuH-7 cells were lysed 72 h later for determination of luciferase activity, according to the luciferase assay system manual (Promega, USA). Data on the number of relative light units (RLU) were used to determine the entry inhibition ratios by use of the CalcuSyn program.

Detection of effects of body fluids on Zaire PsV entry-inhibitory activity of HP-HSA *in vitro*. The effects of mouse serum, rabbit serum, monkey serum, human serum, human SF, or vaginal fluid simulant (VFS) were determined as previously described (46, 53). Briefly, HP-HSA was diluted in these body fluids or DMEM as a control to a concentration of 50 μM, followed by preincubation at 37°C for 1 h. The mixtures were then serially diluted with DMEM to test and calculate entry-inhibitory activity against Zaire PsV as described above. Especially, the above-described mixtures which contained serum were incubated at 56°C for 30 min before the entry inhibition assay was performed.

Detection of *ex vivo* Zaire PsV entry-inhibitory activity of HP-HSA. The animal experiment protocol was reviewed and approved by the Animal Experiment Committee of the School of Basic Medical Sciences, Fudan University (approval number 20160927-1). Eight-week-old female ICR mice (purchased from the Department of Laboratory Animal Science, Fudan University) were divided into four groups. The mice in these groups were intravenously administered PBS, 280 mg/kg HSA, 40 mg/kg HP-HSA, or 280 mg/kg HP-HSA. Serum samples were collected at 1, 5, or 24 h postadministration and serially diluted for Zaire PsV entry inhibition testing. The ratio of the weight change of each mouse was recorded up to day 28 postadministration, at which time euthanasia was performed. Livers and kidneys were collected for microimaging after hematoxylin and eosin (H&E) staining.

Cytotoxicity assay. The cytotoxicity of HP-modified or unmodified HSA to HuH-7 and differentiated THP-1 cells was measured following the instructions in the manual provided in the cell counting kit-8 (CCK-8; Dojindo Molecular Technologies, Japan). Briefly, a series of dilutions of HP-HSA or HSA was mixed with 10,000 HuH-7 cells or 20,000 differentiated THP-1 cells in each well of 96-well plates. After incubation for 48 h, the culture medium was replaced by 100 μl fresh cell medium with 3.5 μl of the solution from CCK-8. After an additional 3 h of incubation at 37°C, the absorbance at 450 nm (A_{450}) of each well was determined as the readout of cell viability.

Thermostability test. HP-HSA buffered by PBS was divided into small stocks and kept at different temperatures (4°C, 25°C, 37°C, and 45°C) for 1, 2, 4, and 8 weeks. Each sample was mixed with Zaire PsV or Sudan PsV at a final concentration of 2.5 μM to assess the entry-inhibitory activity against EBOV PsV. Especially, one stock of HP-HSA was stored at 4°C for 12 months and then serially diluted to test the entry-inhibitory activity of Zaire PsV.

Time-of-addition assay. HuH-7 cells plated in 96-well plates were incubated with Zaire PsV, while HP-HSA at a final concentration of 5 μM was added 30 min before or 0, 0.5, 1, 2, 4, 6, or 8 h after addition of PsV. Cells were lysed 72 h later to determine the entry inhibition ratio.

Time-of-removal assay. HuH-7 cells plated in 96-well plates were previously incubated with 100 μl 5 μM HP-HSA or HSA at 37°C for 1 h and then washed with DMEM 3 times before addition of Zaire PsV. A normal entry inhibition assay with 5 μM HP-HSA or HSA was also performed as a control.

ELISA for protein binding. Eighty nanograms of purified Zaire GP (from which residues 314 to 462 and 637 to 676 were deleted) diluted in PBS was coated onto all wells of a 96-well polystyrene plate (Corning, USA) at 4°C overnight. After blocking with protein-free blocking buffer (Thermo Fisher Scientific, USA), HP-HSA, HSA, MIL77-2, or MIL77-3 serially diluted in PBS was added the wells and the plate was incubated at 37°C for 2 h. Either goat anti- HSA antibody (Abcam, UK) at a 1:1,000 dilution or HRP-conjugated goat anti-human IgG antibody (Abcam, UK) at a 1:3,000 dilution was correspondingly added into the wells with HP-HSA, HSA, or MIL77 antibodies. After incubation at 37°C for 1 h, the absorbance of the wells incubated with MIL77 antibodies (used as a positive control) was measured after reacting with tetramethylbenzidine (Sigma, USA), while the wells incubated with HP-HSA and HSA were further incubated with HRP-conjugated rabbit anti-goat IgG antibody (Dako, Denmark) at a 1:3,000 dilution ratio for one more hour at 37°C before measurement of the absorbance.

Drug combination assay. The synergistic effect of HP-HSA and MIL77 antibodies on Zaire PsV was tested. HP-HSA and MIL77-2 were mixed at their respective 4-fold EC_{50} (the concentration required for 50% of a maximal effect). HP-HSA and MIL77-3 at a concentration of 2.5 μM each were mixed. The mixtures were serially diluted and applied to the entry inhibition assay as described above. The combination index (CI) was calculated by use of the CalcuSyn program.

VLP entry inhibition assay. mCherry-labeled Zaire viruslike particles (VLPs) were prepared and concentrated as described previously (36–38). Additionally, the conformation of Zaire GPs on the surface of VLPs was verified by an ELISA binding assay with MIL77 antibodies as mentioned above. HuH-7 cells or THP-1 cells (treated with PMA at a final concentration of 120 ng/ml) were planted in 24-well chamber slides at 40,000 cells per well 1 day before the addition of VLPs. The concentrated VLPs and a test inhibitor (all the inhibitors were used at a final concentration of 20 μM, and MIL77-2 and MIL77-3 were used in combination) were premixed 1 h before they were added to the cells. The mixtures were incubated with the cells for 6 to 8 h at 37°C in order to facilitate the entry of VLPs adequately. After incubation, the cells were washed with PBS buffer 3 times before they were fixed with 4% paraformaldehyde. The slides were then sealed with DAPI (4′,6-diamidino-2-phenylindole)-containing mounting medium (Thermo Fisher Scientific, USA) and imaged with a Leica SP8 laser scanning confocal microscope (Leica, Germany). Integrated fluorescence density analysis of the captured images was performed with ImageJ software. In order to verify the ratio of VLP entry, the amounts of VLPs entering HuH-7 cells were

also measured by flow cytometry with a BD Accuri C6 flow cytometer (BD Biosciences, USA), and the results were analyzed by the use of FlowJo software.

Temperature shift assay for VLP entry. The HuH-7 cells planted on slides and the VLP-inhibitor mixtures were prechilled at 4°C for 30 min. Then, the cells were incubated with the mixtures at 4°C for 3 h. After the cells were washed with cold PBS buffer 2 times, the cells were further incubated at 37°C for 8 h before fixation and analysis as mentioned above.

Statistical analysis. All drug dose-effect relationships in this study were calculated by use of the CalcuSyn program (54), and one-way analysis of variance was performed with the GraphPad Prism (version 5) program.

SUPPLEMENTAL MATERIAL

Supplemental material for this article may be found at https://doi.org/10.1128/AAC.02168-16.

TEXT S1, PDF file, 5.9 MB.

ACKNOWLEDGMENTS

We are grateful to Xin Zhao, Guangzhou Institute of Biomedicine and Health, Chinese Academy of Sciences, who helped us as a consultant on synthetic chemistry.

We declare no conflicts of interest.

This work was funded by the National Natural Science Foundation of China (81590762) and the National Key Research and Development Program of China (2016YFC1201000, 2016YFC1200405, and 2016YFC1202901).

The funders had no role in study design, data collection and interpretation, or the decision to submit the work for publication.

REFERENCES

1. Weyer J, Grobbelaar A, Blumberg L. 2015. Ebola virus disease: history, epidemiology and outbreaks. Curr Infect Dis Rep 17:480. https://doi.org/10.1007/s11908-015-0480-y.
2. Feldmann H, Geisbert TW. 2011. Ebola haemorrhagic fever. Lancet 377:849–862. https://doi.org/10.1016/S0140-6736(10)60667-8.
3. Knipe DM, Howley PM, Cohen JI, Griffin DE, Lamb RA, Martin MA, Racaniello VR, Roizman B (ed). 2013. Fields virology, 6th ed. Lippincott Williams & Wilkins, Philadelphia, PA.
4. WHO. 2016. Ebola situation report. WHO, Geneva, Switzerland. http://www.who.int/csr/disease/ebola/en/.
5. Alexander KA, Sanderson CE, Marathe M, Lewis BL, Rivers CM, Shaman J, Drake JM, Lofgren E, Dato VM, Eisenberg MC, Eubank S. 2015. What factors might have led to the emergence of Ebola in West Africa? PLoS Negl Trop Dis 9:e0003652. https://doi.org/10.1371/journal.pntd.0003652.
6. de La Vega MA, Caleo G, Audet J, Qiu X, Kozak RA, Brooks JI, Kern S, Wolz A, Sprecher A, Greig J, Lokuge K, Kargbo DK, Kargbo B, Di Caro A, Grolla A, Kobasa D, Strong JE, Ippolito G, Van Herp M, Kobinger GP. 2015. Ebola viral load at diagnosis associates with patient outcome and outbreak evolution. J Clin Invest 125:4421–4428. https://doi.org/10.1172/JCI83162.
7. Lanini S, Portella G, Vairo F, Kobinger GP, Pesenti A, Langer M, Kabia S, Brogiato G, Amone J, Castilletti C, Miccio R, Zumla A, Capobianchi MR, Di Caro A, Strada G, Ippolito G, INMI-EMERGENCY EBOV Sierra Leone Study Group. 2015. Blood kinetics of Ebola virus in survivors and nonsurvivors. J Clin Invest 125:4692–4698. https://doi.org/10.1172/JCI83111.
8. Sow MS, Etard JF, Baize S, Magassouba N, Faye O, Msellati P, Toure AI, Savane I, Barry M, Delaporte E, Postebogui Study Group. 2016. New evidence of long-lasting persistence of Ebola virus genetic material in semen of survivors. J Infect Dis 214:1475–1476. https://doi.org/10.1093/infdis/jiw078.
9. Deen GF, Knust B, Broutet N, Sesay FR, Formenty P, Ross C, Thorson AE, Massaquoi TA, Marrinan JE, Ervin E, Jambai A, McDonald SL, Bernstein K, Wurie AH, Dumbuya MS, Abad N, Idriss B, Wi T, Bennett SD, Davies T, Ebrahim FK, Meites E, Naidoo D, Smith S, Banerjee A, Erickson BR, Brault A, Durski KN, Winter J, Sealy T, Nichol ST, Lamunu M, Stroher U, Morgan O, Sahr F. 14 October 2015. Ebola RNA persistence in semen of Ebola virus disease survivors—preliminary report. N Engl J Med. https://doi.org/10.1056/NEJMoa1511410.
10. Mate SE, Kugelman JR, Nyenswah TG, Ladner JT, Wiley MR, Cordier-Lassalle T, Christie A, Schroth GP, Gross SM, Davies-Wayne GJ, Shinde SA, Murugan R, Sieh SB, Badio M, Fakoli L, Taweh F, de Wit E, van Doremalen N, Munster VJ, Pettitt J, Prieto K, Humrighouse BW, Stroher U, DiClaro JW, Hensley LE, Schoepp RJ, Safronetz D, Fair J, Kuhn JH, Blackley DJ, Laney AS, Williams DE, Lo T, Gasasira A, Nichol ST, Formenty P, Kateh FN, De Cock KM, Bolay F, Sanchez-Lockhart M, Palacios G. 2015. Molecular evidence of sexual transmission of Ebola virus. N Engl J Med 373:2448–2454. https://doi.org/10.1056/NEJMoa1509773.
11. Li H, Ying T, Yu F, Lu L, Jiang S. 2015. Development of therapeutics for treatment of Ebola virus infection. Microbes Infect 17:109–117. https://doi.org/10.1016/j.micinf.2014.11.012.
12. Qiu X, Wong G, Audet J, Bello A, Fernando L, Alimonti JB, Fausther-Bovendo H, Wei H, Aviles J, Hiatt E, Johnson A, Morton J, Swope K, Bohorov O, Bohorova N, Goodman C, Kim D, Pauly MH, Velasco J, Pettitt J, Olinger GG, Whaley K, Xu B, Strong JE, Zeitlin L, Kobinger GP. 2014. Reversion of advanced Ebola virus disease in nonhuman primates with ZMapp. Nature 514:47–53. https://doi.org/10.1038/nature13777.
13. Flyak AI, Shen X, Murin CD, Turner HL, David JA, Fusco ML, Lampley R, Kose N, Ilinykh PA, Kuzmina N, Branchizio A, King H, Brown L, Bryan C, Davidson E, Doranz BJ, Slaughter JC, Sapparapu G, Klages C, Ksiazek TG, Saphire EO, Ward AB, Bukreyev A, Crowe JE, Jr. 2016. Cross-reactive and potent neutralizing antibody responses in human survivors of natural Ebolavirus infection. Cell 164:392–405. https://doi.org/10.1016/j.cell.2015.12.022.
14. Humphreys G. 2011. Vaccination: rattling the supply chain. Bull World Health Organ 89:324–325. https://doi.org/10.2471/BLT.11.030511.
15. Hey A. 2015. History and practice: antibodies in infectious diseases. Microbiol Spectr 3:AID-0026-2014. https://doi.org/10.1128/microbiolspec.AID-0026-2014.
16. Soka MJ, Choi MJ, Baller A, White S, Rogers E, Purpura LJ, Mahmoud N, Wasunna C, Massaquoi M, Abad N, Kollie J, Dweh S, Bemah PK, Christie A, Ladele V, Subah OC, Pillai S, Mugisha M, Kpaka J, Kowalewski S, German E, Stenger M, Nichol S, Stroher U, Vanderende KE, Zarecki SM, Green HH, Bailey JA, Rollin P, Marston B, Nyenswah TG, Gasasira A, Knust B, Williams D. 2016. Prevention of sexual transmission of Ebola in Liberia through a national semen testing and counselling programme for survivors: an analysis of Ebola virus RNA results and behavioural data. Lancet Glob Health 4:e736–e743. https://doi.org/10.1016/S2214-109X(16)30175-9.
17. Uyeki TM, Erickson BR, Brown S, McElroy AK, Cannon D, Gibbons A, Sealy T, Kainulainen MH, Schuh AJ, Kraft CS, Mehta AK, Lyon GM, III, Varkey JB, Ribner BS, Ellison RT, III, Carmody E, Nau GJ, Spiropoulou C, Nichol ST,

Stroher U. 2016. Ebola virus persistence in semen of male survivors. Clin Infect Dis 62:1552–1555. https://doi.org/10.1093/cid/ciw202.
18. Johansen LM, DeWald LE, Shoemaker CJ, Hoffstrom BG, Lear-Rooney CM, Stossel A, Nelson E, Delos SE, Simmons JA, Grenier JM, Pierce LT, Pajouhesh H, Lehar J, Hensley LE, Glass PJ, White JM, Olinger GG. 2015. A screen of approved drugs and molecular probes identifies therapeutics with anti-Ebola virus activity. Sci Transl Med 7:290ra289. https://doi.org/10.1126/scitranslmed.aaa5597.
19. Sissoko D, Laouenan C, Folkesson E, M'Lebing AB, Beavogui AH, Baize S, Camara AM, Maes P, Shepherd S, Danel C, Carazo S, Conde MN, Gala JL, Colin G, Savini H, Bore JA, Le Marcis F, Koundouno FR, Petitjean F, Lamah MC, Diederich S, Tounkara A, Poelart G, Berbain E, Dindart JM, Duraffour S, Lefevre A, Leno T, Peyrouset O, Irenge L, Bangoura N, Palich R, Hinzmann J, Kraus A, Barry TS, Berette S, Bongono A, Camara MS, Chanfreau Munoz V, Doumbouya L, Souley H, Kighoma PM, Koundouno FR, Rene L, Loua CM, Massala V, Moumouni K, Provost C, Samake N, Sekou C, et al. 2016. Experimental treatment with favipiravir for Ebola virus disease (the JIKI trial): a historically controlled, single-arm proof-of-concept trial in Guinea. PLoS Med 13:e1001967. https://doi.org/10.1371/journal.pmed.1001967.
20. Vogel G, Kupferschmidt K. 2015. In setback for potential Ebola drug, company halts trial. Science. https://doi.org/10.1126/science.aac6876.
21. Smith LM, Hensley LE, Geisbert TW, Johnson J, Stossel A, Honko A, Yen JY, Geisbert J, Paragas J, Fritz E, Olinger G, Young HA, Rubins KH, Karp CL. 2013. Interferon-beta therapy prolongs survival in rhesus macaque models of Ebola and Marburg hemorrhagic fever. J Infect Dis 208:310–318. https://doi.org/10.1093/infdis/jis921.
22. Geisbert TW, Hensley LE, Jahrling PB, Larsen T, Geisbert JB, Paragas J, Young HA, Fredeking TM, Rote WE, Vlasuk GP. 2003. Treatment of Ebola virus infection with a recombinant inhibitor of factor VIIa/tissue factor: a study in rhesus monkeys. Lancet 362:1953–1958. https://doi.org/10.1016/S0140-6736(03)15012-X.
23. Sun Z, Wang Q, Jia R, Xia S, Li Y, Liu Q, Xu W, Xu J, Du L, Lu L, Jiang S. 2015. Intranasal administration of maleic anhydride-modified human serum albumin for pre-exposure prophylaxis of respiratory syncytial virus infection. Viruses 7:798–819. https://doi.org/10.3390/v7020798.
24. Lu L, Yang X, Li Y, Jiang S. 2013. Chemically modified bovine beta-lactoglobulin inhibits human papillomavirus infection. Microbes Infect 15:506–510. https://doi.org/10.1016/j.micinf.2013.03.003.
25. Li L, He L, Tan S, Guo X, Lu H, Qi Z, Pan C, An X, Jiang S, Liu S. 2010. 3-Hydroxyphthalic anhydride-modified chicken ovalbumin exhibits potent and broad anti-HIV-1 activity: a potential microbicide for preventing sexual transmission of HIV-1. Antimicrob Agents Chemother 54:1700–1711. https://doi.org/10.1128/AAC.01046-09.
26. Guo X, Qiu L, Wang Y, Wang Y, Wang Q, Song L, Li Y, Huang K, Du X, Fan W, Jiang S, Wang Q, Li H, Yang Y, Meng Y, Zhu Y, Lu L, Jiang S. 2016. A randomized open-label clinical trial of an anti-HPV biological dressing (JB01-BD) administered intravaginally to treat high-risk HPV infection. Microbes Infect 18:148–152. https://doi.org/10.1016/j.micinf.2015.10.004.
27. Neurath AR, Jiang S, Strick N, Lin K, Li YY, Debnath AK. 1996. Bovine beta-lactoglobulin modified by 3-hydroxyphthalic anhydride blocks the CD4 cell receptor for HIV. Nat Med 2:230–234. https://doi.org/10.1038/nm0296-230.
28. Guo X, Qiu L, Wang Y, Wang Y, Meng Y, Zhu Y, Lu L, Jiang S. 2016. Safety evaluation of chemically modified beta-lactoglobulin administered intravaginally. J Med Virol 88:1098–1101. https://doi.org/10.1002/jmv.24439.
29. Lee JE, Fusco ML, Hessell AJ, Oswald WB, Burton DR, Saphire EO. 2008. Structure of the Ebola virus glycoprotein bound to an antibody from a human survivor. Nature 454:177–182. https://doi.org/10.1038/nature07082.
30. Murin CD, Fusco ML, Bornholdt ZA, Qiu X, Olinger GG, Zeitlin L, Kobinger GP, Ward AB, Saphire EO. 2014. Structures of protective antibodies reveal sites of vulnerability on Ebola virus. Proc Natl Acad Sci U S A 111:17182–17187. https://doi.org/10.1073/pnas.1414164111.
31. Qiu X, Audet J, Lv M, He S, Wong G, Wei H, Luo L, Fernando L, Kroeker A, Fausther Bovendo H, Bello A, Li F, Ye P, Jacobs M, Ippolito G, Saphire EO, Bi S, Shen B, Gao GF, Zeitlin L, Feng J, Zhang B, Kobinger GP. 2016. Two-mAb cocktail protects macaques against the Makona variant of Ebola virus. Sci Transl Med 8:329ra333. https://doi.org/10.1126/scitranslmed.aad9875.
32. Saeed MF, Kolokoltsov AA, Albrecht T, Davey RA. 2010. Cellular entry of Ebola virus involves uptake by a macropinocytosis-like mechanism and subsequent trafficking through early and late endosomes. PLoS Pathog 6:e1001110. https://doi.org/10.1371/journal.ppat.1001110.
33. Wang H, Shi Y, Song J, Qi J, Lu G, Yan J, Gao GF. 2016. Ebola viral glycoprotein bound to its endosomal receptor Niemann-Pick C1. Cell 164:258–268. https://doi.org/10.1016/j.cell.2015.12.044.
34. Kuroda M, Fujikura D, Nanbo A, Marzi A, Noyori O, Kajihara M, Maruyama J, Matsuno K, Miyamoto H, Yoshida R, Feldmann H, Takada A. 2015. Interaction between TIM-1 and NPC1 is important for cellular entry of Ebola virus. J Virol 89:6481–6493. https://doi.org/10.1128/JVI.03156-14.
35. Hunt CL, Lennemann NJ, Maury W. 2012. Filovirus entry: a novelty in the viral fusion world. Viruses 4:258–275. https://doi.org/10.3390/v4020258.
36. Manicassamy B, Rong L. 2009. Expression of Ebolavirus glycoprotein on the target cells enhances viral entry. Virol J 6:75. https://doi.org/10.1186/1743-422X-6-75.
37. Shoemaker CJ, Schornberg KL, Delos SE, Scully C, Pajouhesh H, Olinger GG, Johansen LM, White JM. 2013. Multiple cationic amphiphiles induce a Niemann-Pick C phenotype and inhibit Ebola virus entry and infection. PLoS One 8:e56265. https://doi.org/10.1371/journal.pone.0056265.
38. Anantpadma M, Kouznetsova J, Wang H, Huang R, Kolokoltsov A, Guha R, Lindstrom AR, Shtanko O, Simeonov A, Maloney DJ, Maury W, LaCount DJ, Jadhav A, Davey RA. 2016. Large-scale screening and identification of novel Ebola virus and Marburg virus entry inhibitors. Antimicrob Agents Chemother 60:4471–4481. https://doi.org/10.1128/AAC.00543-16.
39. Kouznetsova J, Sun W, Martinez-Romero C, Tawa G, Shinn P, Chen CZ, Schimmer A, Sanderson P, McKew JC, Zheng W, Garcia-Sastre A. 2014. Identification of 53 compounds that block Ebola virus-like particle entry via a repurposing screen of approved drugs. Emerg Microbes Infect 3:e84. https://doi.org/10.1038/emi.2014.88.
40. Tran EE, Nelson EA, Bonagiri P, Simmons JA, Shoemaker CJ, Schmaljohn CS, Kobinger GP, Zeitlin L, Subramaniam S, White JM. 2016. Mapping of Ebolavirus neutralization by monoclonal antibodies in the ZMapp cocktail using cryo-electron tomography and studies of cellular entry. J Virol 90:7618–7627. https://doi.org/10.1128/JVI.00406-16.
41. Aleksandrowicz P, Marzi A, Biedenkopf N, Beimforde N, Becker S, Hoenen T, Feldmann H, Schnittler HJ. 2011. Ebola virus enters host cells by macropinocytosis and clathrin-mediated endocytosis. J Infect Dis 204(Suppl 3):S957–S967. https://doi.org/10.1093/infdis/jir326.
42. Mercer J, Helenius A. 2009. Virus entry by macropinocytosis. Nat Cell Biol 11:510–520. https://doi.org/10.1038/ncb0509-510.
43. Gordon DJ, Boyer JL, Korn ED. 1977. Comparative biochemistry of non-muscle actins. J Biol Chem 252:8300–8309.
44. He Y, Ning T, Xie T, Qiu Q, Zhang L, Sun Y, Jiang D, Fu K, Yin F, Zhang W, Shen L, Wang H, Li J, Lin Q, Li H, Zhu Y, Yang D. 2011. Large-scale production of functional human serum albumin from transgenic rice seeds. Proc Natl Acad Sci U S A 108:19078–19083. https://doi.org/10.1073/pnas.1109736108.
45. Giritch A, Marillonnet S, Engler C, van Eldik G, Botterman J, Klimyuk V, Gleba Y. 2006. Rapid high-yield expression of full-size IgG antibodies in plants coinfected with noncompeting viral vectors. Proc Natl Acad Sci U S A 103:14701–14706. https://doi.org/10.1073/pnas.0606631103.
46. Li L, Qiao P, Yang J, Lu L, Tan S, Lu H, Zhang X, Chen X, Wu S, Jiang S, Liu S. 2010. Maleic anhydride-modified chicken ovalbumin as an effective and inexpensive anti-HIV microbicide candidate for prevention of HIV sexual transmission. Retrovirology 7:37. https://doi.org/10.1186/1742-4690-7-37.
47. Dias JM, Kuehne AI, Abelson DM, Bale S, Wong AC, Halfmann P, Muhammad MA, Fusco ML, Zak SE, Kang E, Kawaoka Y, Chandran K, Dye JM, Saphire EO. 2011. A shared structural solution for neutralizing ebolaviruses. Nat Struct Mol Biol 18:1424–1427. https://doi.org/10.1038/nsmb.2150.
48. Johnson JC, Martinez O, Honko AN, Hensley LE, Olinger GG, Basler CF. 2014. Pyridinyl imidazole inhibitors of p38 MAP kinase impair viral entry and reduce cytokine induction by Zaire Ebolavirus in human dendritic cells. Antiviral Res 107:102–109. https://doi.org/10.1016/j.antiviral.2014.04.014.
49. Empig CJ, Goldsmith MA. 2002. Association of the caveola vesicular system with cellular entry by filoviruses. J Virol 76:5266–5270. https://doi.org/10.1128/JVI.76.10.5266-5270.2002.
50. Chan SY, Speck RF, Ma MC, Goldsmith MA. 2000. Distinct mechanisms of entry by envelope glycoproteins of Marburg and Ebola (Zaire) viruses. J Virol 74:4933–4937. https://doi.org/10.1128/JVI.74.10.4933-4937.2000.
51. Li W, Yu F, Wang Q, Qi Q, Su S, Xie L, Lu L, Jiang S. 2016. Co-delivery of HIV-1 entry inhibitor and nonnucleoside reverse transcriptase inhibitor shuttled by nanoparticles: cocktail therapeutic strategy for

antiviral therapy. AIDS 30:827–838. https://doi.org/10.1097/QAD.0000000000000971.
52. Zhu Y, Lu L, Xu L, Yang H, Jiang S, Chen YH. 2010. Identification of a gp41 core-binding molecule with homologous sequence of human TNNI3K-like protein as a novel human immunodeficiency virus type 1 entry inhibitor. J Virol 84:9359–9368. https://doi.org/10.1128/JVI.00644-10.
53. Fernandez-Romero JA, Thorn M, Turville SG, Titchen K, Sudol K, Li J, Miller T, Robbiani M, Maguire RA, Buckheit RW, Jr, Hartman TL, Phillips DM. 2007. Carrageenan/MIV-150 (PC-815), a combination microbicide. Sex Transm Dis 34:9–14. https://doi.org/10.1097/01.olq.0000223287.46097.4b.
54. Chou TC, Talalay P. 1984. Quantitative analysis of dose-effect relationships: the combined effects of multiple drugs or enzyme inhibitors. Adv Enzyme Regul 22:27–55. https://doi.org/10.1016/0065-2571(84)90007-4.
55. Sekula B, Ciesielska A, Rytczak P, Koziolkiewicz M, Bujacz A. 2016. Structural evidence of the species-dependent albumin binding of the modified cyclic phosphatidic acid with cytotoxic properties. Biosci Rep 36:e00338. https://doi.org/10.1042/BSR20160089.